ASTHMA

Early infancy microbial and metabolic alterations affect risk of childhood asthma

Marie-Claire Arrieta,[1,2]* Leah T. Stiemsma,[2,3]* Pedro A. Dimitriu,[2] Lisa Thorson,[1] Shannon Russell,[1,2] Sophie Yurist-Doutsch,[1,2] Boris Kuzeljevic,[3] Matthew J. Gold,[4] Heidi M. Britton,[1] Diana L. Lefebvre,[5] Padmaja Subbarao,[6,7] Piush Mandhane,[8,9] Allan Becker,[10] Kelly M. McNagny,[4] Malcolm R. Sears,[5] Tobias Kollmann,[3,11] the CHILD Study Investigators,[†] William W. Mohn,[2] Stuart E. Turvey,[3,11‡§] B. Brett Finlay[1,2,12‡§]

Asthma is the most prevalent pediatric chronic disease and affects more than 300 million people worldwide. Recent evidence in mice has identified a "critical window" early in life where gut microbial changes (dysbiosis) are most influential in experimental asthma. However, current research has yet to establish whether these changes precede or are involved in human asthma. We compared the gut microbiota of 319 subjects enrolled in the Canadian Healthy Infant Longitudinal Development (CHILD) Study, and show that infants at risk of asthma exhibited transient gut microbial dysbiosis during the first 100 days of life. The relative abundance of the bacterial genera *Lachnospira*, *Veillonella*, *Faecalibacterium*, and *Rothia* was significantly decreased in children at risk of asthma. This reduction in bacterial taxa was accompanied by reduced levels of fecal acetate and dysregulation of enterohepatic metabolites. Inoculation of germ-free mice with these four bacterial taxa ameliorated airway inflammation in their adult progeny, demonstrating a causal role of these bacterial taxa in averting asthma development. These results enhance the potential for future microbe-based diagnostics and therapies, potentially in the form of probiotics, to prevent the development of asthma and other related allergic diseases in children.

INTRODUCTION

Asthma is a chronic inflammatory disease of the airways currently affecting more than 300 million people worldwide (*1*, *2*). It is also the most prevalent childhood disease in westernized countries (*1*, *2*), highlighting the marked disparity in prevalence between developed and developing countries (*3*). Like other immune-mediated diseases, asthma pathogenesis has genetic and environmental components. Genome-wide association studies have yielded several gene loci associated with asthma, but these do not explain the largest proportion of asthma heritability (*4*). Epidemiologic studies have found a number of environmental exposures associated with asthma that may better explain the sharp increase in asthma prevalence in the past 30 years. Many of these exposures are associated with early-life events known to alter the microbiota, including pre- and perinatal antibiotics, delivery by caesarean section, urban (versus farm) living, and formula feeding (*5*). The microflora hy-

pothesis suggests the intestinal microbiota as the link between these environmental changes and our immune system, and many recent studies have identified the intestinal microbiota as a potential therapeutic target in the prevention of asthma and atopic disease (*6*–*9*). There is now evidence in mice and humans of an early-life "critical window" in which the effects of gut microbial dysbiosis are most influential in human immune development (*10*–*12*). We recently showed that perinatal antibiotic treatment of ovalbumin (OVA)–challenged (asthma-induced) mice exacerbates airway inflammation by increasing serum and surface-bound immunoglobulin E (IgE) and decreasing regulatory T cell (T_{reg}) accumulation in the colon (*11*). Research associating these early-life gut microbial changes with asthma development, however, has not yet been translated into humans.

Early life gut microbial alterations not only are limited to shifts in the prevalence of gut microbes (*10*, *11*) but also include changes in the production of microbial-derived metabolites such as short-chain fatty acids (SCFAs) (*13*) and other metabolites that interact with host immune cells (*13*–*15*). Recently, the SCFAs acetate and propionate were implicated in the reduction of airway cellular infiltration in a mouse model of lung inflammation (*13*). Shifts in SCFAs have also been associated with the development of food allergies in children (*16*). In addition, by measuring a complete set of small-molecule metabolites, also known as the metabolome, recent studies have detected several metabolites associated with asthma in both humans (*17*) and guinea pigs (*18*). This metabolic signal involves metabolites of host and bacterial origin (*17*), both of which are important in asthma pathogenesis. However, to our knowledge, there is no current research aimed to detect early-life metabolic changes before asthma diagnosis that can potentially be used as biomarkers to predict or avert disease development.

Designed to elucidate the factors involved in asthma and atopic disease development, the Canadian Healthy Infant Longitudinal Development (CHILD) Study is a multicenter, longitudinal, prospective, general

[1]Michael Smith Laboratories, University of British Columbia, Vancouver, British Columbia V6T 1Z4, Canada. [2]Department of Microbiology & Immunology, University of British Columbia, Vancouver, British Columbia V6T 1Z3, Canada. [3]Child & Family Research Institute and BC Children's Hospital, Vancouver, British Columbia V4Z 4H4, Canada. [4]Biomedical Research Centre, University of British Columbia, Vancouver, British Columbia V6T 1Z3, Canada. [5]Department of Medicine, McMaster University, Hamilton, Ontario L8S 4L8, Canada. [6]Department of Pediatrics, University of Toronto, Toronto, Ontario M5S 2J7, Canada. [7]Hospital for Sick Children, Toronto, Ontario M5G 1X8, Canada. [8]Department of Pediatrics, University of Alberta, Edmonton, Alberta T6G 2R3, Canada. [9]School of Public Health, University of Alberta, Edmonton, Alberta T6G 2R3, Canada. [10]Department of Pediatrics and Child Health, University of Manitoba, Winnipeg, Manitoba R3T 2N2, Canada. [11]Department of Pediatrics, University of British Columbia, Vancouver, British Columbia V6T 1Z4, Canada. [12]Department of Biochemistry and Molecular Biology, University of British Columbia, Vancouver, British Columbia V6T 1Z4, Canada.
*These authors contributed equally to this work.
†CHILD Study Investigators are listed in the Supplementary Materials.
‡These authors contributed equally to this work.
§Corresponding author. E-mail: sturvey@cw.bc.ca (S.E.T.); bfinlay@mail.ubc.ca (B.B.F.)

population birth cohort study following infants from pregnancy until 5 years of age. Here, we provide evidence in a cohort of 319 human subjects enrolled in the CHILD Study supporting a link between gut microbial dysbiosis in the first 100 days of life, characterized by reductions in four bacterial genera—*Lachnospira*, *Veillonella*, *Faecalibacterium*, and *Rothia*—and an increased risk to develop asthma. We confirmed this association in a mouse model of experimental asthma and showed that supplementation with these bacterial taxa ameliorated lung inflammation in previously germ-free mice inoculated with stool from an asthmatic patient. Additionally, we performed an in-depth analysis of the functional potential of the gut microbiota, combined with the measurement of fecal SCFAs and urinary metabolomic analysis. This comprehensive analysis provides an understanding of early-life alterations in microbial and host metabolism that precede asthma development in children.

RESULTS

Assessment of asthma risk in CHILD Study subjects

Using a nested case-control design, we selected 319 children from the CHILD Study for gut microbiome analysis (see Materials and Methods for the inclusion and exclusion criteria). The study participants were grouped into four clinically distinct phenotypes based on allergy skin prick testing (that is, atopy) and clinical wheeze data at 1 year of age: atopy + wheeze (AW, $n = 22$), atopy only ($n = 87$), wheeze only ($n = 136$), and controls ($n = 74$) (Fig. 1). Given that the CHILD Study is longitudinal, over the course of this study, the children in this cohort reached 3 years of age, and thus, 2- and 3-year clinical data were used to confirm the clinical significance of the 1-year phenotypes. We applied the stringent Asthma Predictive Index (API), a clinically validated predictive index for the presence of active asthma at school age (between 6 and 13 years of age) (19). A positive API at 3 years of age is associated with a 77% chance of active asthma at school age, whereas children assigned a negative API have only a 3% chance of experiencing active asthma at school
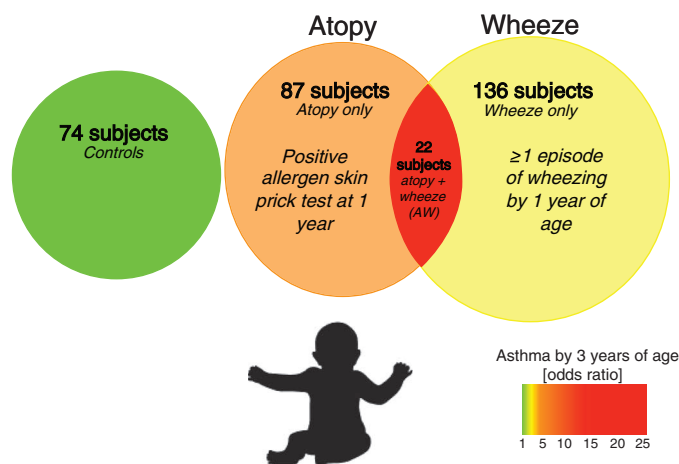

Fig. 1. Classification of study participants. Distribution of 319 subjects among the four 1-year clinical phenotypes based on skin prick tests and wheeze data at 1 year of age: controls, AW, atopy only, and wheeze only. The odds ratios (ORs) associating the phenotypes to a 3-year asthma diagnosis are signified as a heatmap color relative to the control group [ORs: AW versus controls, 21.5 ($P = 0.0022$; 95% CI, 2.4 to 196.0); atopy only versus controls, 5.4 (ns); wheeze only versus controls, 4.0 (ns)].

age (20). CHILD Study subjects in the AW group at 1 year of age were 13.5 times more likely [$P = 0.0003$; 95% confidence interval (CI), 3.2 to 57.4] than the controls, 5.6 times ($P = 0.0037$; 95% CI, 1.8 to 17.5) more likely than the atopy only group, and 4.9 times ($P = 0.0036$; 95% CI, 1.8 to 14) more likely than the wheeze only group to have a positive API. Children were also assessed by a CHILD clinician at 3 years of age for the diagnosis of asthma. The AW group was 21.5 times more likely than the control group ($P = 0.002$; 95% CI, 2.4 to 196.0), 3.9 times more likely than the atopy only group ($P = 0.0429$; 95% CI, 1.09 to 14.5), and 5.4 times more likely than the wheeze only group ($P = 0.0137$; 95% CI, 1.5 to 19.0) to be diagnosed with asthma by 3 years of age (Fig. 1). Together, the API and diagnosis of asthma at 3 years of age emphasize the clinical relevance of the AW phenotype at age 1 year.

In line with other asthma epidemiologic studies (21), exact logistic regression analysis identified antibiotic exposure in the first year of life (OR, 5.6; $P = 0.009$) and atopic dermatitis (see Definitions of clinical variables in Materials and Methods for definition) at 1 year (OR, 6.4; $P = 0.005$) as factors that increased a subject's risk of being classified in the AW group compared to controls (table S1). Caesarean birth (22), exclusive formula feeding (22), and antibiotic exposure (23) in infancy are also common factors associated with gut microbial dysbiosis, but only antibiotic exposure in the first year of life was found to be a significant factor in this subpopulation.

Gut microbiome changes in infants at risk of asthma

Consistent with microbiome studies in other cohorts of young children (24), principal components analysis (PCA) identified age as the main driver of microbial and metabolic shifts in this cohort (figs. S1 and S2 and table S2). Overall gut community composition did not differ substantially among clinical phenotypes, as shown by PCA of the 3-month and 1-year samples (Fig. 2A and fig. S3A). Additionally, although previous studies have shown a decrease in microbial diversity in fecal samples from asthmatic patients (25), our study did not reveal any significant differences in diversity among the four phenotypes (Fig. 2B and fig. S3B). Nevertheless, a comparison of relative taxa abundance according to the clinical phenotype (Fig. 2C) identified differences in the prevalence of some less abundant bacterial taxa (that is, Micrococcaceae and Veillonellaceae) in the 3-month stool samples, differences that were not present at 1 year (fig. S3C). These differences were even more apparent at the genus level (fig. S4, A and B), where the AW group exhibited lower abundances of the genera *Faecalibacterium*, *Lachnospira*, *Rothia*, and *Veillonella*, exclusively at 3 months. Statistical analysis of the top 50 operational taxonomic units (OTUs) across phenotypes yielded 8 differentially abundant OTUs at 3 months, including the genera *Faecalibacterium*, *Lachnospira*, *Rothia*, *Veillonella*, and *Peptostreptococcus*, whereas only 1 OTU was differentially abundant at 1 year, *Oscillospira* (table S3; mt test, raw $P = 0.03$). Comparison of relative taxa abundances among atopic versus non-atopic or wheezing versus non-wheezing children did not identify any significant differences in the 3-month or 1-year gut microbiota (figs. S6 and S7). This, and the significantly increased likelihood of the AW subjects to be diagnosed with asthma by 3 years of age, prompted validation of 16S sequence data among the two extreme phenotypes (AW and controls) using quantitative polymerase chain reaction (qPCR).

We designed and optimized specific primers for the genera *Faecalibacterium*, *Lachnospira*, *Rothia*, *Veillonella*, and *Bifidobacterium*. A subset of samples ($n_{AW} = 21$, $n_{CTRL3-months} = 20$, $n_{CTRL1-year} = 19$), representative of the original cohort ($n_{AW} = 22$, $n_{control} = 74$) based on an exact logistic regression model (table S9), was selected for qPCR based on criteria

specified in Materials and Methods. qPCR confirmed significantly lower abundances of *Veillonella*, *Lachnospira*, *Rothia*, and *Faecalibacterium* in the 3-month AW stool samples compared to controls (Fig. 2D; Mann-Whitney, *P* < 0.001). The abundance of *Bifidobacterium*, a taxon with similar relative abundance in AW and controls, was also measured to further validate the consistency between the 16*S* and the qPCR results. In agreement with the 16*S* sequencing results, these differences were much less apparent in the 1-year stool [*Veillonella* and *Lachnospira* showed less significant differences (*P* < 0.05), whereas the other three genera were not significantly different], suggesting that reductions in these genera are associated with atopy and wheezing by 1 year of age. Further, because the children in the AW phenotype are 21.5 times more likely than the control group to develop asthma by 3 years of age (Fig. 1), these results suggest that lower abundances of these bacterial taxa in early life are associated with a high risk of asthma diagnosis by 3 years of age.

Microbe-derived functional changes in infants at high risk of asthma

To determine the importance of this early-life dysbiosis in the infants at highest risk of asthma, the functional potential of the fecal microbiota was predicted using
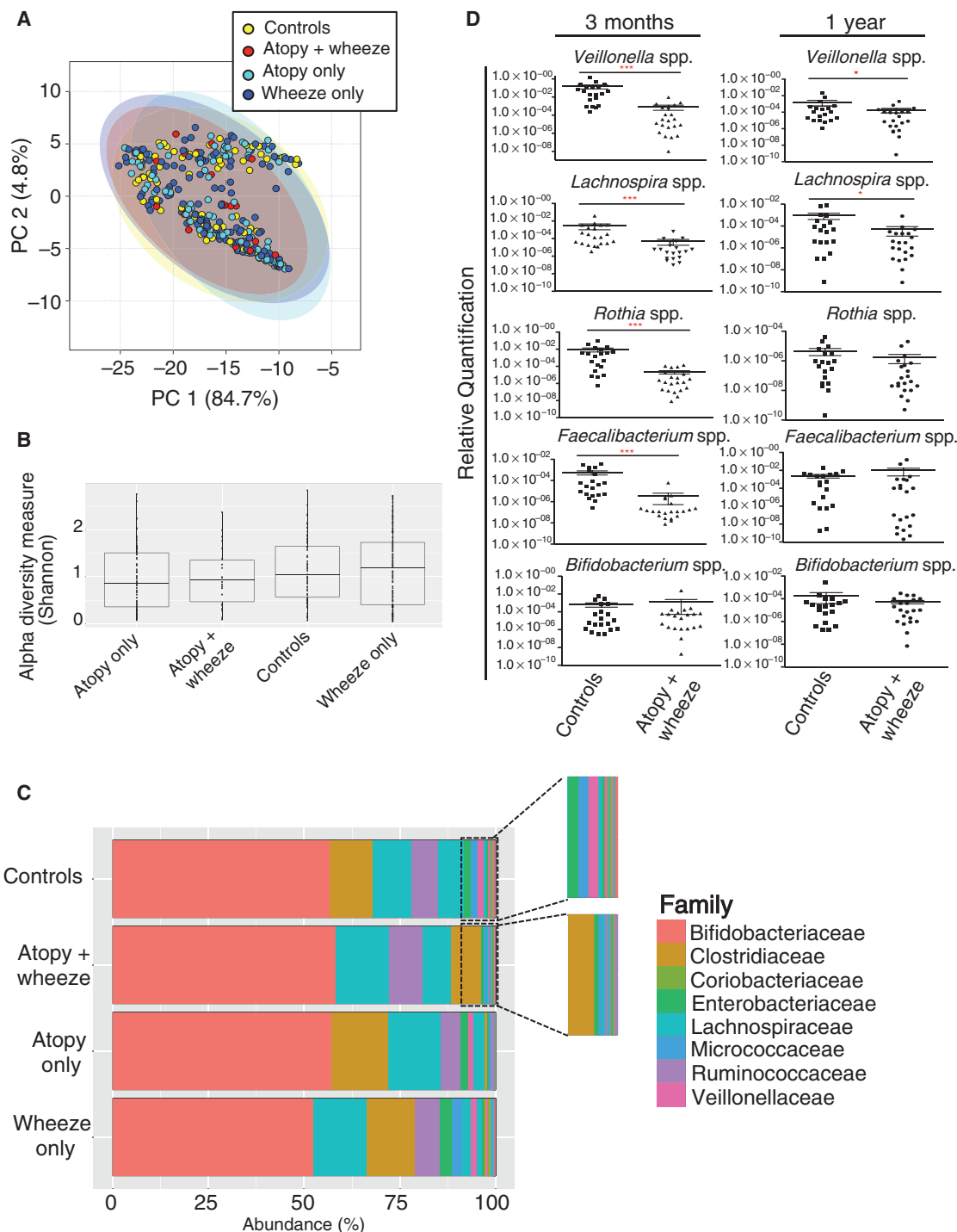

Fig. 2. Gut microbial composition and functional potential by clinical phenotype at 3 months. (**A**) Multivariate analysis by PCA of the fecal microbiota across the four clinical phenotypes at 3 months. Circles denote 95% CIs. (**B**) Alpha diversity (Shannon diversity index) among the four clinical phenotypes at 3 months [shown as box plots, the upper and lower "hinges" correspond to the first and third quartiles (the 25th and 75th percentiles)]. (**C**) Relative abundance of bacterial families within the top 100 OTUs among the four phenotypes at 3 months. Colors of rectangles correspond to the bacterial families in the legend. Rectangles represent specific OTUs, which are organized in order of abundance. (**D**) qPCR quantification of selected genera relative to total 16*S* amplification in all AW fecal samples and a randomly selected subset of control fecal samples at 3 months ($n_{CTRL} = 20$, $n_{AW} = 21$) and 1 year ($n_{CTRL} = 19$, $n_{AW} = 21$) (Graphs based on a logarithmic scale, * < 0.05, ** < 0.01, *** < 0.001. Mann-Whitney; *Veillonella*: $P_{3mo} = 0.0001$, $P_{1y} = 0.0368$; *Lachnospira*: $P_{3mo} = 0.0002$, $P_{1y} = 0.029$; *Rothia*: $P_{3mo} = 0.0001$, $P_{1y} =$ ns; *Faecalibacterium*: $P_{3mo} = 0.0001$, $P_{1y} =$ ns; *Bifidobacterium*: $P_{3mo} =$ ns, $P_{1y} =$ ns).

Fig. 3. PICRUSt analysis at 3 months and 1 year of age. (**A** and **B**) Heatmap of the top 30 most significant differentially abundant genes (KOs) between AW and controls at (A) 3 months and (B) 1 year obtained by PICRUSt analysis of the same subset of samples in Fig. 2D ($n_{AW} = 21$, $n_{CTRL3-months} = 20$, $n_{CTRL1-year} = 19$). Heatmap colors represent variance-stabilized KO abundance (red, low abundance; green, high abundance). KO identification can be found in additional data table S1. Hierarchical clustering of the subjects was based on Euclidean distance using the complete linkage method.

PICRUSt (Phylogenetic Investigation of Communities by Reconstruction of Unobserved States), an algorithm that infers the functional metagenome of microbial communities based on marker gene data and reference bacterial genomes. We compared the inferred genetic composition of the fecal microbiota in the same subset of samples selected for qPCR (Fig. 3) and observed a number of genes that were associated with the AW phenotype. Of the total 6911 genes [defined as KEGG (Kyoto Encyclopedia of Genes and Genomes) orthologs (KO)] surveyed, 2364 genes were significantly different at 3 months, whereas only 125 genes were different at 1 year [additional data table S1; Wald test and false discovery rate (FDR), $P < 0.05$]. The top 30 differential genes (based on lowest P values; table S4) highlight the capacity of these genes to discriminate between the AW group and controls at 3 months, but not at 1 year of age (Fig. 3). This functional difference in the 3-month stool samples suggests potential for the community to influence development of asthma. The functional differences in the AW community involved genes with diverse metabolic functions (that is, gene replication, carbon metabolism, transporters, and amino acid biosynthesis; table S5). Once these genes were organized into specific metabolic pathways, lipopolysaccharide (LPS) biosynthesis was the pathway that differed most between the AW and control groups (Welch's t test, fig. S5A). To validate this result, LPS was extracted and quantified in stool samples available for analysis. Consistent with the PICRUSt predictions, the LPS concentration was lower in the feces of AW children ($n_{AW} = 14$, $n_{CTRL} = 12$; Mann-Whitney, $P = 0.09$; fig. S5B). These biochemical data support the PICRUSt-predicted results, suggesting a real functional change in bacterial composition. Consistent with the importance of changes very early in life, significant differences in specific metabolic pathways between the clinical groups were not found in the 1-year samples.

The functional implications of the gut community in AW children were further investigated by measuring SCFA levels in feces and
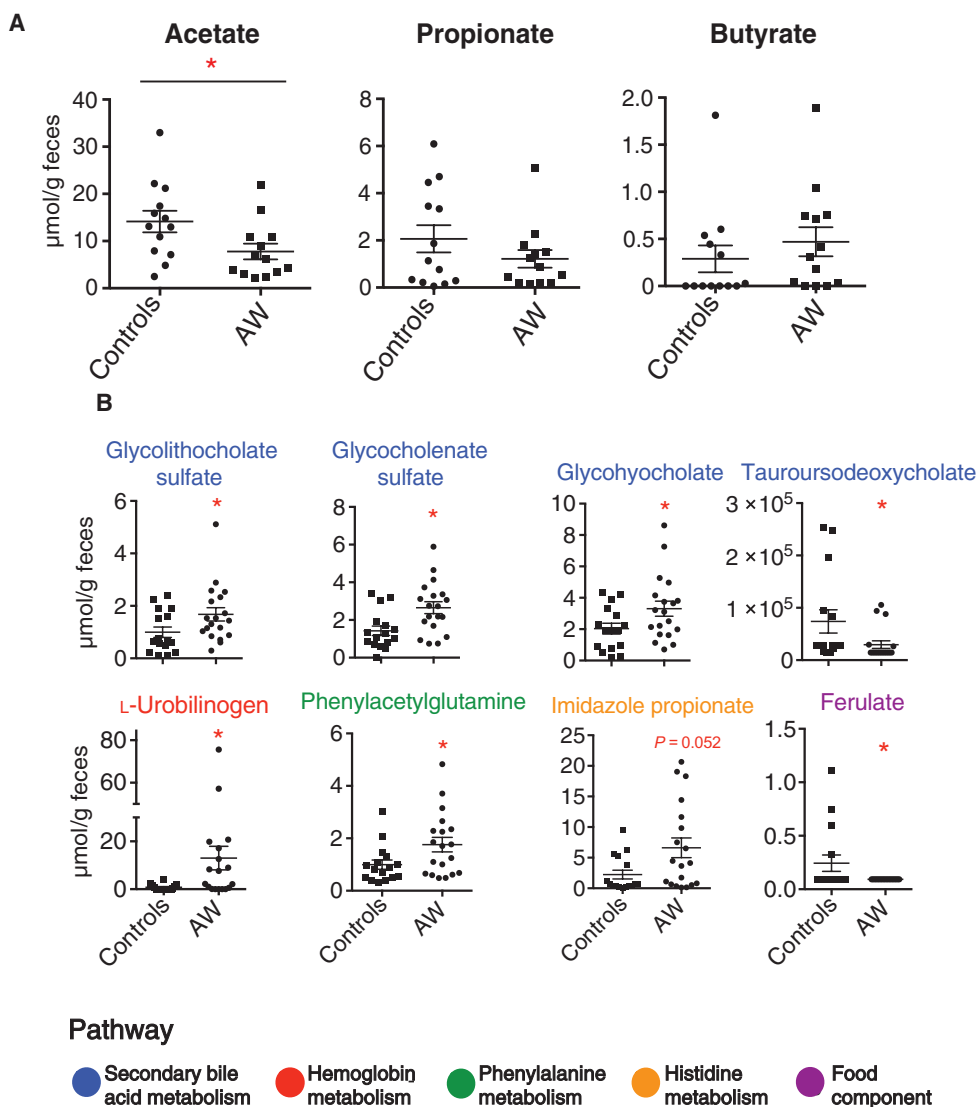
A
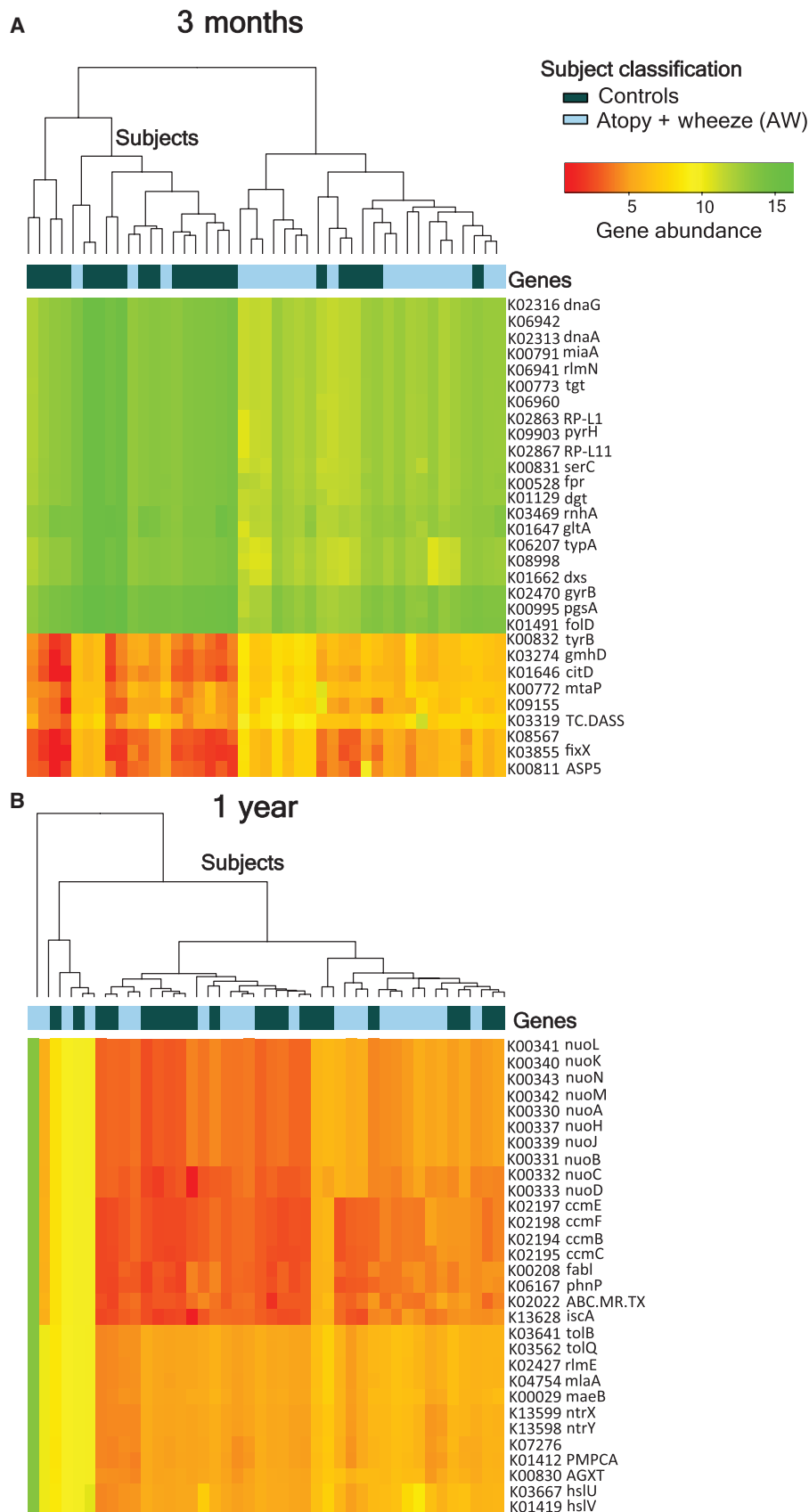
Fig. 4. Metabolites in feces and urine at 3 months of age. (**A**) Concentration of the three most abundant SCFAs in feces of AW and control samples at 3 months of age, measured by gas chromatography (GC) and normalized to feces wet weight (n_{AW} = 13, $n_{control}$ = 13; Mann-Whitney, P = 0.03 for acetate). (**B**) Relative concentration of metabolites of known microbial origin or contribution detected in the urine of AW and control samples at 3 months of age. Metabolomics data are shown as scaled intensities normalized to osmolality, measured by ultrahigh performance liquid chromatography–tandem mass spectrometry (UPLC-MS/MS). The color of the plot titles denotes the biochemical pathway in which the metabolite is involved (n_{AW} = 19, $n_{control}$ = 16; Mann-Whitney, P = 0.048, 0.006, 0.047, 0.049, 0.0264, 0.0334, 0.052, and 0.0394, respectively: * < 0.05).

urine, as well by urine metabolomics. An exact logistic regression model was used to confirm that the control and AW subsets used for SCFA and metabolomics analyses were representative of the larger cohort (n_{AW} = 22, $n_{control}$ = 74) (tables S10 to S13). At 3 months of age, fecal samples of AW children had a significantly lower concentration of acetate (Fig. 4A and table S6). A biweight correlation analysis between the top 50 OTUs organized into families and acetate did not show any significant correlations between specific taxa and acetate. This could be because the ability to ferment 6-carbon sugars and produce this SCFA is shared by several bacterial species belonging to phylogenetically distant taxa, or due to a difference in acetate intestinal uptake.

Urine metabolomic analysis was used to identify metabolic differences of both host and microbial origin (26). By comparing urine from AW and control subjects, a subtle yet significant metabolic signal was detected between the two phenotypes (of the 580 metabolites identified, 39 differed significantly at 3 months and 28 differed at 1 year). Given our focus on the microbiome, we examined metabolites of microbial origin or contribution. Eight metabolites influenced by bacterial metabolism were differentially excreted in the urine of AW children compared to controls at 3 months of age, whereas only two were differentially detected at 1 year, reflecting once again the impact of microbial dysbiosis in early infancy. At 3 months, the excretion of sulfated bile acids glycolithocholate, glycocholenate, and glycohyocholate was higher in AW children, whereas tauroursodeoxycholate excretion was decreased (Fig. 4B). Perhaps the most striking metabolic difference observed in the urine of AW children was the 14-fold increase in urobilinogen, a specific product of the gut microbiota. Urobilinogen is formed by the reduction of bilirubin, a breakdown product of heme catabolism. Correlation analysis did not find significant associations between microbial taxa and these metabolic changes. Thus, it is possible that the alterations in these urinary metabolites are the result of a combination of microbial and host metabolic activity. Nevertheless, they constitute a marker of gut dysbiosis in early infancy that can be detected in urine and that is linked to asthma risk.

FLVR-mediated amelioration of murine lung inflammation

To move from correlation to causation, the role of *Faecalibacterium* sp., *Lachnospira* sp., *Veillonella* sp., and *Rothia* sp. (collectively abbreviated as FLVR) in asthma susceptibility was explored in a murine model of airway inflammation with humanized microbiota. Adult germ-free (GF) mice (n = 4) were inoculated with feces from one AW subject collected at 3 months or with the same human inoculum deliberately supplemented with live FLVR. This AW subject was chosen on the basis of the very low abundance of these four taxa in the 3-month feces, the positive stringent API, and the formal diagnosis of asthma by 3 years of age. The fecal microbiota from the subsequent generation (F1) was clearly distinguishable between mice born to parents supplemented with FLVR or not (Fig. 5A). Mice born to parents harboring FLVR successfully maintained these strains, with *Lachnospira* sp. colonizing at a much higher abundance than the other three strains (Fig. 5, B and C).

PICRUSt analysis from these microbial communities yielded 138 significantly different pathways between the AW and AW + FLVR groups (additional data table S2; Welch's t test and FDR, $P < 0.05$). This large functional change was expected given the striking differences between the two gut microbial communities. Secondary bile acid metabolism and carbohydrate metabolism—pathways that were also altered in the urine of AW children—were among the differential pathways in this experiment (fig. S8A). Additionally, the concentration of the SCFA butyrate (not acetate) was reduced in the AW mouse group, indicating that SCFA production was also increased in mice upon FLVR inoculation (fig. S8B). The difference in SCFA alterations between mice and humans may be explained by the differences in microbial populations between the two species. Similarly, the interspecies differences in gut microbial populations may explain the PICRUSt-predicted decrease in LPS pathways in mice treated with FLVR (fig. S8A). The biggest difference in microbial population between mice and humans was the presence of Bacteroidetes OTUs in mice. Unlike the fecal microbial communities in 3-month-old children, mice given the AW microbiota had a large proportion of Bacteroidetes OTUs (Gram-negative, LPS-positive), which were substituted mainly by *Lachnospira* sp. (Gram-positive, LPS-negative) upon FLVR treatment.

To determine whether FLVR supplementation would modulate an airway inflammatory response, the F1 generation was immunized with OVA at 7 to 8 weeks of age. Mice inoculated with the AW microbiota exhibited a severe lung inflammatory response to OVA, characterized by a mixed lung infiltrate composed of neutrophils, eosinophils, macrophages, and lymphocytes. However, supplementation of the AW microbiota with FLVR significantly decreased the total lung cell infiltrate, as well as the total number of neutrophils and lymphocytes in the bronchoalveolar lavage (BAL; $P < 0.05$) (Fig. 5, D and E). Biweight correlation analysis showed that *Lachnospira* has a strong negative correlation with total BAL cell counts ($r = -0.82$, adjusted $P = 0.009$), whereas the other two bacterial species that were also significantly correlated were much less abundant and had lower correlation values (fig. S9). Histopathological scoring confirmed that supplementation with FLVR reduced airway inflammation (Fig. 5, F and G; $P < 0.01$). In addition, FLVR supplementation significantly reduced both the concentrations of the proinflammatory cytokines [interferon-γ (IFN-γ), tumor necrosis factor (TNF), interleukin-17A (IL-17A), and IL-6] in lung homogenates and OVA-specific IgG2a levels in serum (fig. S10, A and B; $P < 0.01$ to 0.0001). Together, these data show that the microbiota from the AW sample induced a mixed T helper cell 1 (T_H1)/T_H2/T_H17 lung inflammatory response, and that deliberate, therapeutic colonization with FLVR significantly reduced the T_H1/T_H17 components of the immune response.

DISCUSSION

Our findings indicate that in humans, the first 100 days of life represent an early-life critical window in which gut microbial dysbiosis is linked to the risk of asthma and allergic disease. These findings are consistent with previous animal studies (*11, 27, 28*). This early-life microbial dysbiosis is characterized by reductions in four specific bacterial genera—*Faecalibacterium, Lachnospira, Veillonella,* and *Rothia*—rather than changes in overall community composition or diversity, which have been observed in previous studies (*25*). Further, our data also show that these gut microbial changes are much less apparent by 1 year of age, suggesting that therapeutic interventions to address microbial dysbiosis

would need to occur very early in life. Future work in similar human cohorts surveying additional time points over the course of the first year of life will help determine with better accuracy the range of time where this dysbiosis can be detected and its dynamics.

Enhanced appreciation of the human microbiome has revealed that a compositional difference in bacterial communities does not necessarily translate to functional differences (*29*). We addressed this potential disconnect by inferring metagenomic information from the 16S data, as well as by measuring SCFA and urine metabolites. PICRUSt analysis showed LPS biosynthesis pathways to be significantly reduced in AW subjects at 3 months. Considering that the vast majority of the intestinal bacteria detected at 3 months were Gram-positive (all except Enterobacteriaceae and Veillonellaceae), it is possible that the difference in *Veillonella* species may account for the difference in LPS biosynthesis genes in the AW group. The immune status of the children enrolled in this cohort was not studied at 3 months of age due to the challenge of obtaining blood samples at this age. However, LPS exposure has been determined as relevant in the regulation of T_H2-type immune responses by inducing proliferation of IL-12–producing dendritic cells and promoting the T_H1 arm of the immune response (*30*). It has also been demonstrated that diminished exposure of LPS in neonatal mice born via caesarean section prevented the development of tolerance in intestinal immune cells (*31*). Thus, such a marked reduction in one of the only intestinal bacterial groups that produce LPS during early life may have profound immune consequences.

Another important finding of this study is that fecal acetate was significantly reduced in AW subjects at 3 months of age. In animal models of asthma, the SCFAs, propionate (*13*), acetate (*13*), and butyrate (*32*) have all been shown to protect against airway inflammation, and this protective effect has been attributed to the stimulation of T_{regs} and dendritic cells capable of preventing T_H2-type immune responses (*14*). A reduction in glycan metabolism pathways, many of which lead to SCFA production, in AW subjects was also inferred by metagenomic analysis using PICRUSt (table S5), strengthening the association between the gut microbial communities in AW subjects and the measured reduction in fecal acetate.

Other microbe-derived metabolites altered in AW subjects were found in their urine, and these may have potential as early-life biomarkers of asthma risk. These include the secondary bile acids glycolithocholate, glycocholenate, glycohyocholate, and tauroursodeoxycholate. Changes in the urinary excretion of these enterohepatic metabolites can occur from an increase in host production and/or a change in the microbial enzymatic activity on their substrates. Although our study was not designed to unravel the complex mechanisms linking gut microbial dysbiosis with the detected metabolic alterations, it is possible that a reduction in four bacterial taxa known to have enzymatic activity on bile (*33–36*) may induce a change in their urinary excretion. Future work should aim to explore the role of these metabolites in asthma pathogenesis and to determine their biomarker potential in larger human cohorts.

The therapeutic inoculation of GF mice with FLVR significantly reduced airway inflammation in their adult offspring, highlighting the strong immunomodulatory capacity of particular gut microbiota in lung inflammation. FLVR treatment successfully colonized F1 mice with *Lachnospira* and to a lesser extent with *Faecalibacterium, Rothia,* and *Veillonella*. Moreover, there was a significant negative correlation with *Lachnospira* and total BAL counts, strongly suggesting that the reduced inflammatory effect may be due to the presence of *Lachnospira*.

Fig. 5. FLVR-induced attenuation of murine airway inflammation. (**A**) Multivariate analysis by PCA of the fecal microbiota of F1 mice (3-week-old pups) born from parents inoculated with feces of an AW 3-month-old infant (AW), or with the same sample plus a live mixture of *Lachnospira multipara*, *Veillonella parvula*, *Rothia mucilaginosa*, and *Faecalibacterium prausnitzii* (AW + FLVR). Circles denote 95% CIs. (**B**) Bacterial family relative abundance in the same mice in (A). (**C**) The percent abundance of *Lachnospira* sp., *Veillonella* sp., *Rothia* sp., and *Faecalibacterium* sp. was elevated in mouse pups born to parents inoculated with FLVR (green bars). (**D**) Cellular counts in the BAL of mice (AW or AW + FLVR) after a 3-week OVA immunization regime to induce airway inflammation. (**E**) Total cell differential counts in the BAL. Stars denote a significant decrease in lymphocytes (green) and neutrophils (red) between the AW and AW + FLVR groups. (**F** and **G**) Total histopathological scores (F) and representative hematoxylin and eosin–stained lung sections (G). Scale bar, 300 μm. (D to F) $n_{naïve} = 8$, $n_{AW} = 18$, $n_{AW+FLVR} = 28$, analysis of variance (ANOVA); * < 0.05, ** < 0.01, *** < 0.001, **** < 0.0001; for raw data and *P* values, see additional data table S3.
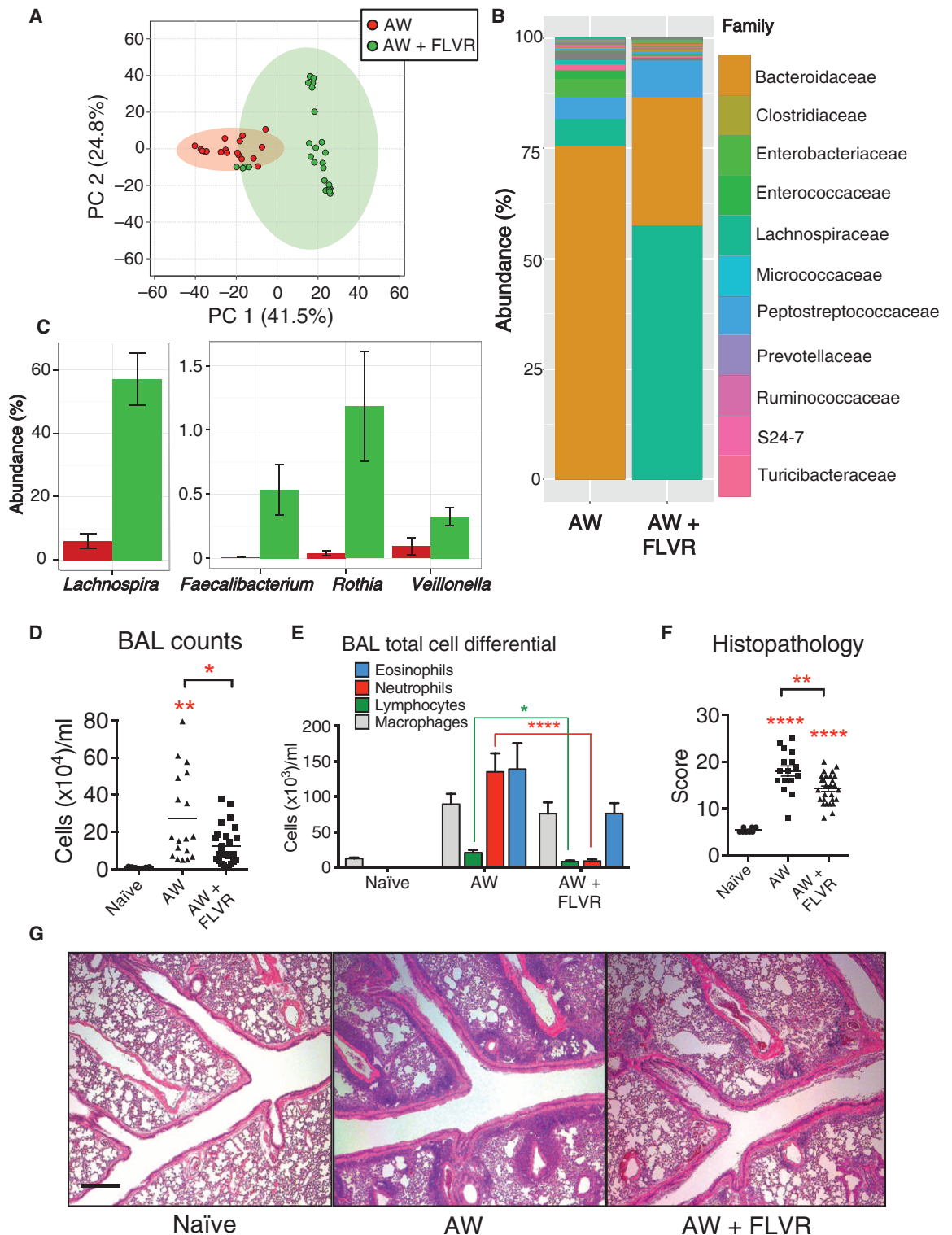
Given the complexity of reproducing human infant microbiota in mice, it was expected that the proportional abundances of FLVR in mice would differ from human control subjects. The adopted gut microbiota observed in the offspring of FLVR-treated mice, as well as the significant reduction in lung inflammation, may be a consequence of *Lachnospira* outcompeting the other three bacteria in FLVR, as well as other bacteria in the AW inoculum. Some, but not all, functional aspects of what was detected in AW human samples were replicated in the mouse experiment, and the lack of complete replication between species is likely due to the large differences in microbial communities between mice and

humans. However, the fact that FLVR supplementation was protective and induced a marked reduction in lung inflammation in mice emphasizes that these taxa are immunomodulatory and involved in asthma.

The cell types that were significantly reduced by FLVR treatment were neutrophils and lymphocytes. Although a reduction in eosinophilia and IgE was not observed, FLVR treatment significantly reduced relevant T_H1/T_H17 immune factors, such as IL-6, IL-17A, and TNF. Notably, the cytokine pattern observed in AW-treated mice is reminiscent of the elevated TNF, IL-17A, and IL-6 associated with severe human asthma with increased levels of neutrophils (37–39).

This study involves the largest human infant cohort for which gut microbial composition and functional potential have been assessed in the context of atopy, wheeze, and asthma. However, repeated and longitudinal exploration in large-scale human cohorts beginning ideally before 3 months of age will be necessary to further confirm the universality of our findings. Further, given that 16S ribosomal RNA (rRNA) sequencing provides researchers with only a compositional analysis of the microbiota, metagenomic sequencing in a similar cohort would provide a more in-depth view of the compositional and functional changes among atopic/asthmatic and healthy children. Additionally, future human microbiota colonization experiments in mice, aimed to improve the resemblance to human infant microbiota, will help to determine the mechanisms by which FLVR influences asthma development early in life.

Our data support transient early-life microbial dysbiosis as an important factor influencing asthma development, and emphasize the protective role played by four specific bacterial genera: *Faecalibacterium*, *Lachnospira*, *Veillonella*, and *Rothia*. We identified several early-life metabolic alterations with biomarker and therapeutic potential, which will prompt further functional studies to determine their role in asthma pathogenesis. Together, our findings establish an important role for the early-life intestinal microbiota in shaping immune system development, and enhance the potential for using rationally designed microbe-based therapies to prevent the development of asthma and other allergic diseases that begin in childhood.

MATERIALS AND METHODS

Study design
This study was based on a nested case-control design to analyze the fecal microbiota of infants enrolled in the CHILD Study (inclusion and exclusion criteria are described below). On the basis of the sample availability, we selected all subjects with 3-month and 1-year stool samples available from the first three phenotypes (AW, atopy only, and wheeze only) and a portion of controls in which additional biological samples were also available. Ultimately, 319 subjects were selected for microbiome analysis. Researchers were blinded to the phenotypic classifications through completion of the Mothur/CrunchClust bioinformatic pipeline. Twenty-two of the 319 subjects selected for microbiome analysis were later determined to be at the highest risk of asthma development (AW), based on the API (19) (described below) and clinician diagnosis of asthma by 3 years of age. The 16S rRNA gene was sequenced from fecal samples collected at 3 and 12 months of age for microbial community composition and diversity analysis. Decreases in four bacterial genera—*Faecalibacterium*, *Lachnospira*, *Veillonella*, and *Rothia* (designated FLVR)—were observed in the AW group compared to the other three phenotypes. To confirm the observed decrease in these four bacterial genera, qPCR was performed in 16S rDNA V3 am-

plicons from all but one of the AW subjects and a randomly chosen subset of 20 control subjects at both time points. One AW subject was excluded because of lack of additional DNA and stool samples, and the control subset was established to be representative of the larger cohort ($n_{control} = 74$) according to an exact logistic regression model (table S9). The potential metagenomic information was obtained from 16S data via PICRUSt analysis in the same subjects chosen for qPCR analysis. To obtain functional metabolic information from the fecal samples, we measured SCFA concentrations at both time points using 13 samples from AW subjects (these were the only remaining samples from the AW subjects). An equal number of controls were also chosen for fecal SCFA measurement from the same subset of samples selected for qPCR analysis. To identify metabolic differences in urine at 3 and 12 months, samples from 16 AW and 19 control subjects were processed for metabolomics analysis, based on the availability of urine samples from the subset originally chosen for qPCR analysis. Although the sample size for both phenotypes (AWs and controls) decreased for SCFA and metabolomics analysis, an exact logistic regression model was used to confirm that the control and AW subsets used for these analyses were representative of the larger cohort. One subject was excluded from this model because of lack of clinical data ($n_{AW} = 21$, $n_{controls} = 74$); however, for other statistical analyses, no human samples were excluded (tables S9 to S13).

On the basis of the findings of the human study, we then tested if the presence of these four bacteria would alter the development of lung inflammation in the OVA experimental mouse model of asthma. This model has been shown to be a good indicator of early-life gut microbe–induced changes in lung inflammation (11, 27). Mice were inoculated with stool from one AW subject or with AW stool + FLVR found to be lower in the human subjects. The mice supplemented with these four bacterial genera displayed significantly decreased lung inflammation. The sample size in animal experiments ($n_{AW} = 18$, $n_{AW+FLVR} = 28$) was based on previous experience with this model. Results are a combination of two separate experiments. Total BAL counts and inflammation scoring were assessed in a blinded fashion. Outliers for mouse experiments were detected and excluded using the ROUT method ($Q = 1\%$) in GraphPad Prism ($n = 1$ to 4).

CHILD Study design, skin prick testing, and sample selection
The CHILD Study is a multicenter longitudinal, prospective, general population birth cohort study following infants from pregnancy to age 5 years, with a total of 3624 pregnant mothers recruited at four sites across Canada (Vancouver, Edmonton, Manitoba, and Toronto). Detailed characteristics of the CHILD Study have been previously described (40–42). Briefly, questionnaires were administered at recruitment, at 36 weeks of gestation, at 3, 6, 12, 18, 24, and 30 months, and at 3, 4, and 5 years. In this way, data are obtained related to environmental exposures, psychosocial stresses, nutrition, and general health. In addition, at ages 1, 3, and 5 years, questionnaires validated in the International Study of Asthma and Allergies in Childhood (ISAAC) (43) are completed by the parent or legal guardian. At age 1, 3, and 5 years, the child is examined for evidence of atopic dermatitis, rhinitis, or asthma. Trained staff performed skin testing using standardized inhalant allergens and common food allergens at 1, 3, and 5 years. Five-year data were not included in this study because it was not available for this entire cohort at the date of submission. Data up to 3 years of age were used for construction of the API and in determining which children were diagnosed with asthma by 3 years of age ($n_{asthma} = 19$, $n_{control} = 300$). The University of British Columbia/Children's and Women's Health Centre of British Columbia

Research Ethics Board approved the research protocols for studies on human samples, and each participating parent or legal guardian gave signed informed consent.

Inclusion/exclusion criteria

Skin prick test results. At 1 year of age, children enrolled in the CHILD Study were tested with 10 allergens (*Alternaria tenuis*, cat hair, dog epithelium, *Dermatophagoides pteronyssinus*, *Dermatophagoides farinae*, German cockroach, peanut, soybean, egg white, and cow's milk). A child was classified as "atopic" if he/she developed a wheal ≥2 mm for any of the 10 allergens tested. Histamine was used as a positive control and glycerin as a negative control. Subjects that tested negative to histamine were not included in this cohort unless they tested positive (with a wheal ≥2 mm) for 1 of the 10 allergens listed above. If a subject tested positive to glycerin, the wheal size for glycerin was subtracted from the wheal size of any positive allergen response.

Wheeze questionnaires. If the child had wheezed with or without a cold during the first year of life (recorded via questionnaires answered by parents at 3, 6, and 12 months), the child was included in the wheezing group. Children were also included in the wheezing group if the CHILD clinician recorded a wheeze during the 1-year clinical assessment.

Biological samples. Both a 3-month and a 1-year stool sample were required for each child to be included in this study. For the control group, subjects from whom additional samples were collected by the CHILD Study (such as blood samples) were selected over subjects missing any of these samples.

Of the 3542 children meeting eligibility criteria at birth, 1427 children had completed the CHILD Study 1-year clinical assessment at the time of selection. A total of 163 subjects were excluded because of incomplete skin prick test data or a positive response to glycerin or a negative response to histamine and all other allergens. The remaining 1264 subjects were grouped into the four clinical phenotypes—AW ($n = 35$), atopy only ($n = 150$), wheeze only ($n = 216$), and controls ($n = 863$)—and assessed for the availability of a 3-month and a 1-year stool sample [n numbers for children with 3-month and 1-year stool samples available: AW ($n = 25$), atopy only ($n = 112$), wheeze only ($n = 179$), and controls ($n = 106$)]. Subjects were then excluded from the study if, after preparation and sequencing of the 16S DNA, the sequence results were inadequate (that is, not enough sequence reads per stool sample) [final n numbers: AW ($n = 22$), atopy only ($n = 87$), wheeze only ($n = 136$), and controls ($n = 74$)]. Informative power calculations are challenging given there is little known about specific links between microbiota and atopic disease, particularly in the current era of bacterial 16S rRNA sequencing.

The subsets of samples for qPCR and PICRUSt analysis included all but one AW sample, and 19 (1 year) or 20 (3 months) randomly selected control samples. Thirteen AW and control samples were submitted for SCFA analysis, and 19 AW and 16 controls were submitted for metabolomics analysis. An exact logistic regression model was used to confirm that all subsets used in this study were representative of the entire cohort ($n_{AW} = 22$, $n_{control} = 74$). The number of samples selected depended on the availability of the fecal or urine samples, which tended to be very limited in this study of human infants.

Asthma Predictive Index

Subjects in the sample cohort ($n = 319$) were also classified according to the API (*19*) ($n_{api} = 33$, $n_{control} = 286$). A positive stringent API is defined by the following criteria: recurrent wheeze between the ages of 2 and 3 years, together with one of two major criteria or two of three minor criteria (see below). Additionally, if a child was diagnosed with asthma at the 3-year clinical assessment, he or she was also included in the positive API group whether or not he or she met the API criteria.

Recurrent wheezing: Recurrent wheezing is defined as ≥3 episodes of wheezing between the ages of 2 and 3 years. Questionnaires at 24 and 30 months, and 3 years of age were used to quantify the number of wheeze episodes between 2 and 3 years.

Major criteria: Parental history of asthma (from either parent) or physician-diagnosed childhood atopic dermatitis between the ages of 2 and 3 years.

Minor criteria: ≥4% eosinophilia, any episodes of wheezing apart from colds after 2 years, and physician-diagnosed allergic rhinitis at 3 years of age.

Definitions of clinical variables

Antibiotic exposure from birth to 1 year: "Yes" defined as receiving one or more antibiotics from birth to 1 year of age. "No" defined as having received no antibiotics from birth to 1 year of age.

Antibiotic exposure from birth to 3 months: "Yes" defined as receiving one or more antibiotics from birth to 3 months of age. "No" defined as having received no antibiotics from birth to 3 months of age.

Atopic dermatitis or eczema at 1 year: "Yes" defined as being diagnosed with atopic dermatitis or eczema (a chronic skin disease characterized by itchy, inflamed skin) by a CHILD clinician at the 1-year clinical assessment or a non-CHILD clinician (reported in the 1-year CHILD health questionnaire). "No" defined as no diagnosis.

Atopic dermatitis or eczema at 3 months: "Yes" defined as being diagnosed with atopic dermatitis or eczema (a chronic skin disease characterized by itchy, inflamed skin) by a non-CHILD clinician (reported in the 3-month CHILD health questionnaire). "No" defined as no diagnosis.

Feeding methods (at 1 year): "Breast-fed" defined as breast-fed for the first 12 months of life (as reported by parents in the 1-year CHILD nutrition questionnaire). "Not breast-fed" defined as breast-fed for less than 12 months of age.

Feeding methods (at 3 months): "Breast-fed" defined as breast-fed for the first 3 months of life (as reported by parents in the 3-month CHILD nutrition questionnaire). "Not breast-fed" defined as breast-fed for less than 3 months of age.

16S microbial community analysis

DNA was extracted from ~50 mg of stool. Samples were mechanically lysed using MO BIO dry bead tubes (MO BIO Laboratories) and the FastPrep homogenizer (FastPrep Instrument, MP Biochemicals) before DNA extraction with the Qiagen DNA Stool Mini Kit.

All samples were amplified by PCR in triplicate using barcoded primer pairs flanking the V3 region of the 16S gene (table S7) as previously described (*44*). Each 50 μl of PCR contained 22 μl of water, 25 μl of TopTaq Master Mix, 0.5 μl of each forward and reverse barcoded primer, and 2 μl of template DNA. The PCR program consisted of an initial DNA denaturation step at 95°C for (5 min), 25 cycles of DNA denaturation at 95°C (1 min), an annealing step at 50°C (1 min), an elongation step at 72°C (1 min), and a final elongation step at 72°C (7 min). Controls without template DNA were included to ensure that no contamination occurred. Amplicons were run on a 2% agarose gel to ensure adequate amplification. Amplicons displaying bands at ~160 bp were purified using the illustra GFX PCR DNA Purification kit. Purified samples were

diluted 1:50 and quantified using PicoGreen (Invitrogen) in the TECAN M200 (excitation at 480 nm and emission at 520 nm).

Illumina sequencing. Pooled PCR amplicons were diluted to 20 ng/µl and sequenced at the V3 hypervariable region using Hi-Seq 2000 bidirectional Illumina sequencing and Cluster Kit v4 (Macrogen Inc.). Library preparation was done using TruSeq DNA Sample Prep v2 Kit (Illumina) with 100 ng of DNA sample and QC library by Bioanalyzer DNA 1000 Chip (Agilent).

Bioinformatics. Sequences were preprocessed, denoised, and quality-filtered by size using Mothur (45). Representative sequences were clustered into OTUs using CrunchClust (46) and classified against the Greengenes Database (47) according to 97% similarity. Any OTUs present less than five times among all samples were removed from the analysis.

Quantitative PCR

To validate sequencing results, the abundance of specific intestinal bacterial genera was measured in the 16S ribosomal DNA (rDNA) V3 amplicons using group-specific 16S rRNA gene primers for the following genera: *Lachnospira*, *Veillonella*, *Rothia*, *Faecalibacterium*, and *Bifidobacterium* (table S8). All AW samples and a randomly selected, but representative equal number of control samples were analyzed by qPCR. All reactions were carried out in the 7500 Fast Real-Time System (Applied Biosystems) or the ViiA 7 Real-Time PCR System (Life Technologies Inc.). Each 10-µl reaction contained 5 µl of iQ SYBR Green Supermix (Bio-Rad), 0.1 µl of each forward and reverse primer, 0.8 µl of nuclease-free water, and 4 µl of the V3 amplicon. The qPCR program consisted of an initial step at 95°C (15 min), 40 cycles of 15 s at 94°C, 30 s at 60°C, and 30 s at 72°C, and a final cycle of 95°C at 15 s, 60°C at 1 min, 95°C at 15 s, and 60°C at 15 s. Per primer set, at least two dilutions were run per sample and all dilutions were run in duplicate. Samples were normalized according to the ΔC_T method using total 16S rDNA (eubacteria; table S8) as the reference gene.

PICRUSt

We used PICRUSt (48) to generate a profile of putative functions (via metagenome prediction) from the 16S rRNA OTU data. Predicted metagenomes from the same human samples analyzed by qPCR and from mouse fecal samples were categorized by function at KEGG Orthology level 3. To test for significant differences in functional category abundances between the AW and control samples, we used the Welch's *t* test implementation of STAMP (49). We also tested for differentially abundant metagenomes with DESeq2 (50) under default settings. The test statistics' *P* values were adjusted for multiple testing using the procedure of Benjamini and Hochberg (51) (FDR threshold, 5%).

SCFA analysis

Human and mouse fecal samples were combined with 25% phosphoric acid, vortexed, and centrifuged until a clear supernatant was obtained. Supernatants were submitted for GC analysis to the Department of Agricultural, Food and Nutritional Science of the University of Alberta. Only 13 AW samples contained enough material for this analysis, and 13 additional control samples were randomly selected for this analysis. Samples were analyzed as previously described (52) with modifications. Briefly, samples were combined with 4-methyl-valeric acid as an internal standard, and 0.2 ml was injected into the Bruker SCION 456 gas chromatograph, using a Stabilwax-DA 30-m × 0.53-mm × 0.5-µm column (Restek). A standard solution containing acetic acid, proprionic

acid, isobutyric acid, butyric acid, isovaleric acid, valeric acid, and caproic acid, combined with internal standard, was injected in every run.

The PTV (programmable temperature vaporization) injector and FID (flame ionization detector) detector temperatures were held at 250°C for the entire run. The oven was started at 80°C and immediately ramped to 210°C at 45°C/min, where it was held for 5.11 min. Total run time was 8.00 min. Helium was used at a constant flow of 20.00 ml/min. Sample concentrations were normalized to the wet weight of feces.

Urine metabolomics

Two hundred microliters of urine per subject was submitted to Metabolon Inc. for metabolomic analysis. From the subset of samples selected for qPCR analysis, 19 AW and 16 control urine samples were available for metabolomics analysis. Sample preparation was carried out as described previously (53). Briefly, recovery standards were added before the first step in the extraction process for quality control purposes. Proteins were precipitated for removal with methanol under vigorous shaking for 2 min (Glen Mills Geno/Grinder 2000) followed by centrifugation. The resulting extract was divided into five fractions: one for analysis by UPLC-MS/MS (positive ionization), one for analysis by UPLC-MS/MS (negative ionization), one for the UPLC-MS/MS polar platform (negative ionization), one for analysis by GC-MS, and one sample was reserved for backup.

The following controls were analyzed with the experimental samples: samples generated from a pool of human urine extensively characterized by Metabolon Inc. and a cocktail of standards spiked into every analyzed sample, which allowed instrument performance monitoring. Experimental samples and controls were randomized across the platform run.

MS analysis. Extracts were subjected to either GC-MS or UPLC-MS/MS. The UPLC-MS/MS platform used a Waters ACQUITY UPLC with Waters UPLC BEH C18 2.1 × 100 mm, 1.7-µm columns, and a Thermo Scientific Q Exactive high-resolution/accurate mass spectrometer interfaced with a heated electrospray ionization (HESI-II) source and Orbitrap mass analyzer operated at 35,000 mass resolution. The sample extract was dried and then reconstituted in acidic or basic liquid chromatography–compatible solvents, each of which contained eight or more injection standards at fixed concentrations to ensure injection and chromatographic consistency. Extracts reconstituted in acidic conditions were gradient-eluted using water and methanol containing 0.1% formic acid, whereas the basic extracts, which also used water/methanol, contained 6.5 mM ammonium bicarbonate. A third aliquot was analyzed via negative ionization following elution from a hydrophilic interaction liquid chromatography (HILIC) column (Waters UPLC BEH Amide 2.1 × 150 mm, 1.7 µm) using a gradient consisting of water and acetonitrile with 10 mM ammonium formate. The MS analysis alternated between MS and data-dependent MS^2 scans using dynamic exclusion, and the scan range was from 80 to 1000 mass/charge ratio (*m/z*).

The samples destined for analysis by GC-MS were dried under vacuum desiccation for a minimum of 18 hours before being derivatized under dried nitrogen using bistrimethyl-silyltrifluoroacetamide. Derivatized samples were separated on a 5% diphenyl/95% dimethyl polysiloxane fused silica column (20 m × 0.18 mm internal diameter; 0.18-µm film thickness) with helium as carrier gas and a temperature ramp from 60° to 340°C in a 17.5-min period. All samples were analyzed on a Thermo Finnigan Trace DSQ fast-scanning single-quadrupole MS using electron impact ionization and operated at unit mass resolving power. The scan range was from 50 to 750 *m/z*.

Compound identification, quantification, and data curation. Metabolites were identified by automated comparison of the ion features in the experimental samples to a reference library of chemical standard entries that included retention time, molecular weight (*m/z*), preferred adducts, and in-source fragments, as well as associated MS spectra, and curated by visual inspection for quality control using software developed at Metabolon (*54*). Identification of known chemical entities is based on comparison to metabolomic library entries of purified standards. Commercially available purified standard compounds have been acquired and registered into the software system known as LIMS used for both the UPLC-MS/MS and GC-MS platforms. Peaks were quantified using area under the curve. Raw area counts for each metabolite in each sample were normalized to correct for variation resulting from instrument inter-day tuning differences by the median value for each run day, therefore setting the median value to 1.0 for each run. Missing values were imputed with the observed minimum after normalization. All values were further normalized to the osmolality of each sample.

LPS determination

LPS was extracted and quantified in a subset of 14 AW and 12 control human fecal samples collected at 3 months of age. Samples were weighed and then homogenized using FastPrep homogenizer (FastPrep Instrument, MP Biochemicals) with one small glass bead in each sample. Samples were then centrifuged at low speed (1200*g*) to remove debris, and the supernatant was further centrifuged at high speed (13,000*g*) for 3 min. The pellet was resuspended in 100 μl of endotoxin-free phosphate-buffered saline (PBS). LPS was extracted by the phenol-chloroform method using an extraction kit (Intron). The extract was used to determine LPS concentration using the limulus amebocyte lysate chromogenic method (Lonza). Samples were run in triplicate, and concentrations were determined using a standard curve and normalized to feces weight.

Human microbiota model of experimental murine allergic asthma

Bacterial inoculum preparation and inoculation. Frozen feces from one AW subject collected at 3 months of age was used to orally inoculate GF mice. A fecal slurry was prepared by scraping a frozen piece of fecal material with a sterile scalpel and combining it with 1 ml of PBS reduced with 0.05% of cysteine-HCl to protect anaerobic species. This type of adoptive transfer has been shown to be effective in transferring human microbiota into mice in our laboratory (unpublished observations) and by others (*55*). The sample was vortexed and centrifuged at 3000*g* to remove debris. Solid cultures of *F. prausnitzii* [American Type Culture Collection (ATCC) 27766], *V. parvula* (ATCC 10790), *R. mucilaginosa* (ATCC 49040), and *L. multipara* (DSM-3073) were grown on fastidious anaerobe (FA) agar at 37°C under anaerobic conditions. One colony of each culture was added to 2 ml of liquid FA medium and grown for 24 hours. The cell concentrations of the fecal slurry and the FLVR culture were calculated by turbidometry at 600 nm and normalized to optical density of 0.3 with reduced PBS.

Four female and four male 6-week-old GF mice (Swiss Webster) were purchased from Taconic. Immediately upon arrival, two female and two male mice were randomly selected to be orally gavaged with 50 μl of the fecal slurry (AW), and the remaining mice were inoculated with 40 μl of the same fecal slurry combined with 10 μl of the FLVR culture. Oral gavages with the microbial treatments were repeated on days 3, 7, and 14 after arrival. After the second inoculation, mice were paired for mating. To further increase the microbial colonization of the F1 mice

with the experimental inocula, the abdominal and nipple areas of the mothers were swabbed with the corresponding bacterial preparations on days 3 and 7 after birth.

Experimental allergic asthma model. Experimental murine allergic asthma was induced in all F1 mice from two subsequent litters for each breeding pair, at 7 to 8 weeks of age, as previously described (*56*) with minor modifications. Although this model does not fully recapitulate the phenotype of human allergic asthma, it is a useful model for evaluating many aspects of this lung inflammatory disease. No statistical methods were used to estimate sample size in animal experiments. A total of 8 control, 18 AW, and 28 AW + FLVR mice were used in the two combined experiments. Mice were sensitized intraperitoneally with 10 μg of grade V OVA and 1.3 mg of aluminum hydroxide (both from Sigma) on days 0 and 7. On days 21, 22, 23, and 24, mice were challenged intranasally with 50 μg of LPS-free OVA in PBS and, on days 25 and 26, with 100 μg of grade V OVA (Sigma). On day 27, mice were anaesthetized with ketamine (200 mg/kg) and xylazine (10 mg/kg), and blood was collected by cardiac puncture. After sacrifice, BALs were performed by 3 × 1 ml washes with PBS. Total BAL counts were blindly assessed by counting cells in a hemocytometer. Eosinophils, neutrophils, macrophages, and lymphocytes were quantified from Cytospins (Thermo Shandon) stained with Hema Stain (Fisher Scientific), based on standard morphological criteria. All protocols used in these experiments were approved by the Animal Care Committee of the University of British Columbia.

Determination of serum OVA-specific Igs

OVA-specific IgE, IgG1, and IgG2a in serum were measured by enzyme-linked immunosorbent assay (Chondrex).

Histology

Lungs were collected and fixed in 10% formalin, embedded in paraffin, cut longitudinally into 5-μm sections, and stained with hematoxylin and eosin. Inflammation was blindly assessed from five fields per section, each graded on a scale of 1 to 5 (1 = no signs of disease, 5 = severe disease) for each of the following four parameters (for a maximum score of 25): (i) peribronchial infiltration, (ii) perivascular infiltration, (iii) parenchymal infiltration, and (iv) epithelium damage.

Cytokines

Lung tissue homogenates were centrifuged twice at 16,000*g*, and the supernatants were stored at −80°C. The levels of IL-2, IL-4, IL-6, IL-10, TNF, IFN-γ, and IL-17A were determined using the Cytometric Bead Array (CBA) assay $T_H1/T_H2/T_H17$ kit (catalog #560485, BD Biosciences). Levels of IL-5, IL-9, and IL-13 were determined by CBA flex set (catalog #558302, 558348, and 558349, BD Biosciences) according to the manufacturer's instructions. Cytokine concentrations were normalized to protein concentration calculated by the Bradford assay (Sigma). IL-9 and IL-13 analysis did not yield results above the sensitivity limit of the assay.

Statistical analysis

An exact logistic regression model based on the Markov chain Monte Carlo sampling (*57–59*) was developed, and ORs were used to evaluate the risk associated with the AW group according to specific clinical data. ORs and the adjusted lower and upper 95% CIs were calculated according to the following formula: $e^{(\ln(OR))}$ and $e^{(\ln(CI))}$, respectively. ln(CI) is equal to the exact upper and lower CIs (table S1). Only subjects

for which all the data were available were included in the model (n_{AW} = 21, $n_{control}$ = 74). This same model was also used to confirm that all subsets of control and AW samples used in this study were representative of the entire cohort (tables S9 to S13). We assessed fecal microbial diversity and the relative abundance of bacterial taxa using phyloseq (60) along with additional R-based computational tools (61–66) in R-studio (R-Studio). PCA was conducted using MetaboAnalyst (67, 68) and statistically confirmed by PERMANOVA (permutational multivariate analysis of variance) (60). The Shannon diversity index was calculated using phyloseq (60) and statistically confirmed by Mann-Whitney (GraphPad Prism software, version 5c). The "mt" function in phyloseq (60) was used to calculate multi-inference–adjusted P values to identify differentially abundant OTUs between the 3-month and 1-year samples and among the four phenotypes: AW, atopy only, wheeze only, and controls. Differences between the control and AW groups were determined by Mann-Whitney for qPCR. All SCFAs and urine metabolites were subject to the Shapiro-Wilk test for normality, and differences between control and AW groups were determined by t test (glycocholenate sulfate and glycohyocholate) or Mann-Whitney. No human samples were excluded from statistical tests. For analyses using human samples, the F test found no significant differences between the variances of the groups. Differences between AW, AW + FLVR, and naïve groups in mice experiments were determined by ANOVA for BAL counts, BAL cell differentials, histology scoring, lung cytokine, and serum immunoglobulin concentrations. All data points in graphs represent biological replicates. Outliers were detected and excluded from mouse experimental data only, using the ROUT method (Q = 1%) in GraphPad Prism (n = 1 to 4). Statistical significance was defined as $P \leq 0.05$.

SUPPLEMENTARY MATERIALS

www.sciencetranslationalmedicine.org/cgi/content/full/7/307/307ra152/DC1
Fig. S1. Gut microbial and host metabolic changes in the first year of life.
Fig. S2. Human gut microbiota at 3 months and 1 year of age.
Fig. S3. One-year-old gut microbiota by clinical phenotype.
Fig. S4. Relative abundance of bacterial genera at (A) 3 months and (B) 1 year.
Fig. S5. PICRUSt-predicted KEGG functional categories.
Fig. S6. Three-month gut microbiota classified by (A) wheeze/non-wheeze or (B) atopy/non-atopy.
Fig. S7. One-year gut microbiota classified by (A) wheeze/non-wheeze or (B) atopy/non-atopy.
Fig. S8. Microbial-derived functional changes in mice treated with FLVR.
Fig. S9. Heatmap of a biweight correlation (bicor) between BAL total cell counts and the top 30 bacterial OTUs from F1 mice feces at 3 weeks of age.
Fig. S10. Lung cytokine concentration and serum concentration of OVA-specific antibodies.
Table S1. Characteristics of the cohort.
Table S2. Differentially abundant OTUs between 3-month and 1-year samples.
Table S3. Differentially abundant taxa among the four clinical phenotypes at 3 months and 1 year.
Table S4. PICRUSt-predicted top 30 differential KOs (based on P value) in AW and controls at 3 months and 1 year.
Table S5. Top 30 biochemical pathways (based on P value) of PICRUSt-predicted KOs in AW and controls at 3 months.
Table S6. SCFAs in feces and urine in AW and controls at 3 months and 1 year.
Table S7. 16S V3 region amplification primers and barcodes.
Table S8. qPCR primer sequences for selected bacterial genera.
Table S9. Exact logistic regression model of qPCR control subset.
Table S10. Exact logistic regression model of metabolomics control subset.
Table S11. Exact logistic regression model of SCFA control subset.
Table S12. Exact logistic regression model of metabolomics AW subset*.
Table S13. Exact logistic regression model of SCFA AW subset*.
Additional Data Tables (separate file)
Additional Data Table S1. PICRUSt-predicted differentially abundant KOs between AW and controls.
Additional Data Table S2. PICRUSt-predicted differentially abundant pathways between AW- and AW + FLVR–treated mice.
Additional Data Table S3. Raw data and P values for all experiments with n < 20.

REFERENCES AND NOTES

1. I. Asher, N. Pearce, Global burden of asthma among children. *Int. J. Tuberc. Lung Dis.* **18**, 1269–1278 (2014).
2. S. T. Holgate, Innate and adaptive immune responses in asthma. *Nat. Med.* **18**, 673–683 (2012).
3. D. Graham-Rowe, Lifestyle: When allergies go west. *Nature* **479**, S2–S4 (2011).
4. F. D. Martinez, D. Vercelli, Asthma. *Lancet* **382**, 1360–1372 (2013).
5. M. C. Arrieta, L. T. Stiemsma, N. Amenyogbe, E. M. Brown, B. Finlay, The intestinal microbiome in early life: Health and disease. *Front. Immunol.* **5**, 427 (2014).
6. J. R. Hunt, R. Martinelli, V. C. Adams, G. A. Rook, L. R. Brunet, Intragastric administration of *Mycobacterium vaccae* inhibits severe pulmonary allergic inflammation in a mouse model. *Clin. Exp. Allergy* **35**, 685–690 (2005).
7. P. Forsythe, M. D. Inman, J. Bienenstock, Oral treatment with live *Lactobacillus reuteri* inhibits the allergic airway response in mice. *Am. J. Respir. Crit. Care Med.* **175**, 561–569 (2007).
8. K. Atarashi, T. Tanoue, T. Shima, A. Imaoka, T. Kuwahara, Y. Momose, G. Cheng, S. Yamasaki, T. Saito, Y. Ohba, T. Taniguchi, K. Takeda, S. Hori, I. I. Ivanov, Y. Umesaki, K. Itoh, K. Honda, Induction of colonic regulatory T cells by indigenous *Clostridium* species. *Science* **331**, 337–341 (2011).
9. A. Shreiner, G. B. Huffnagle, M. C. Noverr, The "microflora hypothesis" of allergic disease. *Adv. Exp. Med. Biol.* **635**, 113–134 (2008).
10. I. C. Arnold, N. Dehzad, S. Reuter, H. Martin, B. Becher, C. Taube, A. Muller, *Helicobacter pylori* infection prevents allergic asthma in mouse models through the induction of regulatory T cells. *J. Clin. Invest.* **121**, 3088–3093 (2011).
11. S. L. Russell, M. J. Gold, B. P. Willing, L. Thorson, K. M. McNagny, B. B. Finlay, Perinatal antibiotic treatment affects murine microbiota, immune responses and allergic asthma. *Gut Microbes* **4**, 158–164 (2013).
12. J. Cahenzli, Y. Koller, M. Wyss, M. B. Geuking, K. D. McCoy, Intestinal microbial diversity during early-life colonization shapes long-term IgE levels. *Cell Host Microbe* **14**, 559–570 (2013).
13. A. Trompette, E. S. Gollwitzer, K. Yadava, A. K. Sichelstiel, N. Sprenger, C. Ngom-Bru, C. Blanchard, T. Junt, L. P. Nicod, N. L. Harris, B. J. Marsland, Gut microbiota metabolism of dietary fiber influences allergic airway disease and hematopoiesis. *Nat. Med.* **20**, 159–166 (2014).
14. N. Arpaia, C. Campbell, X. Fan, S. Dikiy, J. van der Veeken, P. deRoos, H. Liu, J. R. Cross, K. Pfeffer, P. J. Coffer, A. Y. Rudensky, Metabolites produced by commensal bacteria promote peripheral regulatory T-cell generation. *Nature* **504**, 451–455 (2013).
15. B. S. Samuel, A. Shaito, T. Motoike, F. E. Rey, F. Backhed, J. K. Manchester, R. E. Hammer, S. C. Williams, J. Crowley, M. Yanagisawa, J. I. Gordon, Effects of the gut microbiota on host adiposity are modulated by the short-chain fatty-acid binding G protein-coupled receptor, Gpr41. *Proc. Natl. Acad. Sci. U.S.A.* **105**, 16767–16772 (2008).
16. A. Sandin, L. Braback, E. Norin, B. Bjorksten, Faecal short chain fatty acid pattern and allergy in early childhood. *Acta Paediatr.* **98**, 823–827 (2009).
17. E. J. Saude, C. D. Skappak, S. Regush, K. Cook, A. Ben-Zvi, A. Becker, R. Moqbel, B. D. Sykes, B. H. Rowe, D. J. Adamko, Metabolomic profiling of asthma: Diagnostic utility of urine nuclear magnetic resonance spectroscopy. *J. Allergy Clin. Immunol.* **127**, 757–764 (2011).
18. E. J. Saude, I. P. Obiefuna, R. L. Somorjai, F. Ajamian, C. Skappak, T. Ahmad, B. K. Dolenko, B. D. Sykes, R. Moqbel, D. J. Adamko, Metabolomic biomarkers in a model of asthma exacerbation: Urine nuclear magnetic resonance. *Am. J. Respir. Crit. Care Med.* **179**, 25–34 (2009).
19. J. A. Castro-Rodriguez, C. J. Holberg, A. L. Wright, F. D. Martinez, A clinical index to define risk of asthma in young children with recurrent wheezing. *Am. J. Respir. Crit. Care Med.* **162**, 1403–1406 (2000).
20. J. A. Castro-Rodriguez, L. Cifuentes, C. E. Rodriguez-Martinez, The asthma predictive index remains a useful tool to predict asthma in young children with recurrent wheeze in clinical practice. *J. Allergy Clin. Immunol.* **127**, 1082–1083 (2011).
21. L. Hoskin-Parr, A. Teyhan, A. Blocker, A. J. Henderson, Antibiotic exposure in the first two years of life and development of asthma and other allergic diseases by 7.5 yr: A dose-dependent relationship. *Pediatr. Allergy Immunol.* **24**, 762–771 (2013).
22. M. B. Azad, T. Konya, H. Maughan, D. S. Guttman, C. J. Field, R. S. Chari, M. R. Sears, A. B. Becker, J. A. Scott, A. L. Kozyrskyj; on behalf of the CHILD Study Investigators, Gut microbiota of healthy Canadian infants: Profiles by mode of delivery and infant diet at 4 months. *CMAJ* **185**, 385–394 (2013).

23. S. Tanaka, T. Kobayashi, P. Songjinda, A. Tateyama, M. Tsubouchi, C. Kiyohara, T. Shirakawa, K. Sonomoto, J. Nakayama, Influence of antibiotic exposure in the early postnatal period on the development of intestinal microbiota. *FEMS Immunol. Med. Microbiol.* **56**, 80–87 (2009).

24. T. Yatsunenko, F. E. Rey, M. J. Manary, I. Trehan, M. G. Dominguez-Bello, M. Contreras, M. Magris, G. Hidalgo, R. N. Baldassano, A. P. Anokhin, A. C. Heath, B. Warner, J. Reeder, J. Kuczynski, J. G. Caporaso, C. A. Lozupone, C. Lauber, J. C. Clemente, D. Knights, R. Knight, J. I. Gordon, Human gut microbiome viewed across age and geography. *Nature* **486**, 222–227 (2012).

25. T. R. Abrahamsson, H. E. Jakobsson, A. F. Andersson, B. Bjorksten, L. Engstrand, M. C. Jenmalm, Low gut microbiota diversity in early infancy precedes asthma at school age. *Clin. Exp. Allergy* **44**, 842–850 (2014).

26. E. Holmes, J. V. Li, T. Athanasiou, H. Ashrafian, J. K. Nicholson, Understanding the role of gut microbiome–host metabolic signal disruption in health and disease. *Trends Microbiol.* **19**, 349–359 (2011).

27. S. L. Russell, M. J. Gold, M. Hartmann, B. P. Willing, L. Thorson, M. Wlodarska, N. Gill, M. R. Blanchet, W. W. Mohn, K. M. McNagny, B. B. Finlay, Early life antibiotic-driven changes in microbiota enhance susceptibility to allergic asthma. *EMBO Rep.* **13**, 440–447 (2012).

28. T. Olszak, D. An, S. Zeissig, M. P. Vera, J. Richter, A. Franke, J. N. Glickman, R. Siebert, R. M. Baron, D. L. Kasper, R. S. Blumberg, Microbial exposure during early life has persistent effects on natural killer T cell function. *Science* **336**, 489–493 (2012).

29. C. Huttenhower, D. Gevers, R. Knight, S. Abubucker, J. H. Badger, A. T. Chinwalla, H. H. Creasy, A. M. Earl, M. G. FitzGerald, R. S. Fulton, M. G. Giglio, K. Hallsworth-Pepin, E. A. Lobos, R. Madupu, V. Magrini, J. C. Martin, M. Mitreva, D. M. Muzny, E. J. Sodergren, J. Versalovic, A. M. Wollam, K. C. Worley, J. R. Wortman, S. K. Young, Q. D. Zeng, K. M. Aagaard, O. O. Abolude, E. Allen-Vercoe, E. J. Alm, L. Alvarado, G. L. Andersen, S. Anderson, E. Appelbaum, H. M. Arachchi, G. Armitage, C. A. Arze, T. Ayvaz, C. C. Baker, L. Begg, T. Belachew, V. Bhonagiri, M. Bihan, M. J. Blaser, T. Bloom, V. Bonazzi, J. P. Brooks, G. A. Buck, C. J. Buhay, D. A. Busam, J. L. Campbell, S. R. Canon, B. L. Cantarel, P. S. G. Chain, I. M. A. Chen, L. Chen, S. Chhibba, K. Chu, D. M. Ciulla, J. C. Clemente, S. W. Clifton, S. Conlan, J. Crabtree, M. A. Cutting, N. J. Davidovics, C. C. Davis, T. Z. DeSantis, C. Deal, K. D. Delehaunty, F. E. Dewhirst, E. Deych, Y. Ding, D. J. Dooling, S. P. Dugan, W. M. Dunne, A. S. Durkin, R. C. Edgar, R. L. Erlich, C. N. Farmer, R. M. Farrell, K. Faust, M. Feldgarden, V. M. Felix, S. Fisher, A. A. Fodor, L. J. Forney, L. Foster, V. Di Francesco, J. Friedman, D. C. Friedrich, C. C. Fronick, L. L. Fulton, H. Y. Gao, N. Garcia, G. Giannoukos, C. Giblin, M. Y. Giovanni, J. M. Goldberg, J. Goll, A. Gonzalez, A. Griggs, S. Gujja, S. K. Haake, B. J. Haas, H. A. Hamilton, E. L. Harris, T. A. Hepburn, B. Herter, D. E. Hoffmann, M. E. Holder, C. Howarth, K. H. Huang, S. M. Huse, J. Izard, J. K. Jansson, H. Y. Jiang, C. Jordan, V. Joshi, J. A. Katancik, W. A. Keitel, S. T. Kelley, C. Kells, N. B. King, D. Knights, H. D. H. Kong, O. Koren, S. Koren, K. C. Kota, C. L. Kovar, N. C. Kyrpides, P. S. La Rosa, S. L. Lee, K. P. Lemon, N. Lennon, C. M. Lewis, L. Lewis, R. E. Ley, K. Li, K. Liolios, B. Liu, Y. Liu, C. C. Lo, C. A. Lozupone, R. D. Lunsford, T. Madden, A. A. Mahurkar, P. J. Mannon, E. R. Mardis, V. M. Markowitz, K. Mavromatis, J. M. McCorrison, D. McDonald, J. McEwen, A. L. McGuire, P. McInnes, T. Mehta, K. A. Mihindukulasuriya, J. R. Miller, P. J. Minx, I. Newsham, C. Nusbaum, M. O'Laughlin, J. Orvis, I. Pagani, K. Palaniappan, S. M. Patel, M. Pearson, J. Peterson, M. Podar, C. Pohl, K. S. Pollard, M. Pop, M. E. Priest, L. M. Proctor, X. Qin, J. Raes, J. Ravel, J. G. Reid, M. Rho, R. Rhodes, K. P. Riehle, M. C. Rivera, B. Rodriguez-Mueller, Y. H. Rogers, M. C. Ross, C. Russ, R. K. Sanka, P. Sankar, J. F. Sathirapongsasuti, J. A. Schloss, P. D. Schloss, T. M. Schmidt, M. Scholz, L. Schriml, A. M. Schubert, N. Segata, J. A. Segre, W. D. Shannon, R. R. Sharp, T. J. Sharpton, N. Shenoy, N. U. Sheth, G. A. Simone, I. Singh, C. S. Smillie, J. D. Sobel, D. D. Sommer, P. Spicer, G. G. Sutton, S. M. Sykes, D. G. Tabbaa, M. Thiagarajan, C. M. Tomlinson, M. Torralba, T. J. Treangen, R. M. Truty, T. A. Vishnivetskaya, J. Walker, L. Wang, Z. Y. Wang, D. V. Ward, W. Warren, M. A. Watson, C. Wellington, K. A. Wetterstrand, J. R. White, K. Wilczek-Boney, Y. Q. Wu, K. M. Wylie, T. Wylie, C. Yandava, L. Ye, Y. Z. Ye, S. Yooseph, B. P. Youmans, L. Zhang, Y. J. Zhou, Y. M. Zhu, L. Zoloth, J. D. Zucker, B. W. Birren, R. A. Gibbs, S. K. Highlander, B. A. Methe, K. E. Nelson, J. F. Petrosino, G. M. Weinstock, R. K. Wilson, O. White; Human Microbiome Project Consortium, Structure, function and diversity of the healthy human microbiome. *Nature* **486**, 207–214 (2012).

30. T. De Smedt, B. Pajak, E. Muraille, L. Lespagnard, E. Heinen, P. De Baetselier, J. Urbain, O. Leo, M. Moser, Regulation of dendritic cell numbers and maturation by lipopolysaccharide in vivo. *J. Exp. Med.* **184**, 1413–1424 (1996).

31. C. Chassin, M. Kocur, J. Pott, C. U. Duerr, D. Gutle, M. Lotz, M. W. Hornef, miR-146a mediates protective innate immune tolerance in the neonate intestine. *Cell Host Microbe* **8**, 358–368 (2010).

32. M. Fallani, D. Young, J. Scott, E. Norin, S. Amarri, R. Adam, M. Aguilera, S. Khanna, A. Gil, C. A. Edwards, J. Doré; Other members of the INFABIO Team, Intestinal microbiota of 6-week-old infants across Europe: Geographic influence beyond delivery mode, breast-feeding, and antibiotics. *J. Pediatr. Gastroenterol. Nutr.* **51**, 77–84 (2010).

33. E. Jimenez, B. Sanchez, A. Farina, A. Margolles, J. M. Rodriguez, Characterization of the bile and gall bladder microbiota of healthy pigs. *Microbiologyopen* **3**, 937–949 (2014).

34. M. Rogosa, The genus Veillonella. I. General cultural, ecological, and biochemical considerations. *J. Bacteriol.* **87**, 162–170 (1964).

35. N. A. Cornick, N. S. Jensen, D. A. Stahl, P. A. Hartman, M. J. Allison, Lachnospira pectinoschiza sp. nov., an anaerobic pectinophile from the pig intestine. *Int. J. Syst. Bacteriol.* **44**, 87–93 (1994).

36. M. Lopez-Siles, T. M. Khan, S. H. Duncan, H. J. Harmsen, L. J. Garcia-Gil, H. J. Flint, Cultured representatives of two major phylogroups of human colonic Faecalibacterium prausnitzii can utilize pectin, uronic acids, and host-derived substrates for growth. *Appl. Environ. Microbiol.* **78**, 420–428 (2012).

37. M. Manise, G. Holtappels, K. Van Crombruggen, F. Schleich, C. Bachert, R. Louis, Sputum IgE and cytokines in asthma: Relationship with sputum cellular profile. *PLOS One* **8**, e58388 (2013).

38. M. Marini, E. Vittori, J. Hollemborg, S. Mattoli, Expression of the potent inflammatory cytokines, granulocyte-macrophage-colony-stimulating factor and interleukin-6 and interleukin-8, in bronchial epithelial cells of patients with asthma. *J. Allergy Clin. Immunol.* **89**, 1001–1009 (1992).

39. J. C. Virchow Jr., C. Kroegel, C. Walker, H. Matthys, Inflammatory determinants of asthma severity: Mediator and cellular changes in bronchoalveolar lavage fluid of patients with severe asthma. *J. Allergy Clin. Immunol.* **98**, S27–S33 (1996).

40. T. J. Moraes, D. L. Lefebvre, R. Chooniedass, A. B. Becker, J. R. Brook, J. Denburg, K. T. HayGlass, R. G. Hegele, T. R. Kollmann, J. Macri, P. J. Mandhane, J. A. Scott, P. Subbarao, T. K. Takaro, S. E. Turvey, J. D. Duncan, M. R. Sears, A. D. Befus; the CHILD Study Investigators, The Canadian Healthy Infant Longitudinal Development birth cohort study: Biological samples and biobanking. *Paediatr. Perinat. Epidemiol.* **29**, 84–92 (2015).

41. T. K. Takaro, J. A. Scott, R. W. Allen, S. S. Anand, A. B. Becker, A. D. Befus, M. Brauer, J. Duncan, D. L. Lefebvre, W. Lou, P. J. Mandhane, K. E. McLean, G. Miller, H. Sbihi, H. Shu, P. Subbarao, S. E. Turvey, A. J. Wheeler, L. Zeng, M. R. Sears, J. R. Brook; the CHILD Study Investigators, The Canadian Healthy Infant Longitudinal Development (CHILD) birth cohort study: Assessment of environmental exposures. *J. Expo. Sci. Environ. Epidemiol.* 10.1038/jes.2015.7 (2015).

42. P. Subbarao, S. S. Anand, A. B. Becker, A. D. Befus, M. Brauer, J. R. Brook, J. A. Denburg, K. T. HayGlass, M. S. Kobor, T. R. Kollmann, A. L. Kozyrskyj, W. Y. Lou, P. J. Mandhane, G. E. Miller, T. J. Moraes, P. D. Pare, J. A. Scott, T. K. Takaro, S. E. Turvey, J. M. Duncan, D. L. Lefebvre, M. R. Sears; CHILD Study Investigators, The Canadian Healthy Infant Longitudinal Development (CHILD) study: Examining developmental origins of allergy and asthma. *Thorax* **70**, 998–1000 (2015).

43. The International Study of Asthma and Allergies in Childhood (ISAAC) Steering Committee, Worldwide variation in prevalence of symptoms of asthma, allergic rhinoconjunctivitis, and atopic eczema: ISAAC. *Lancet* **351**, 1225–1232 (1998).

44. A. K. Bartram, M. D. Lynch, J. C. Stearns, G. Moreno-Hagelsieb, J. D. Neufeld, Generation of multimillion-sequence 16S rRNA gene libraries from complex microbial communities by assembling paired-end illumina reads. *Appl. Environ. Microbiol.* **77**, 3846–3852 (2011).

45. P. D. Schloss, S. L. Westcott, T. Ryabin, J. R. Hall, M. Hartmann, E. B. Hollister, R. A. Lesniewski, B. B. Oakley, D. H. Parks, C. J. Robinson, J. W. Sahl, B. Stres, G. G. Thallinger, D. J. Van Horn, C. F. Weber, Introducing mothur: Open-source, platform-independent, community-supported software for describing and comparing microbial communities. *Appl. Environ. Microbiol.* **75**, 7537–7541 (2009).

46. M. Hartmann, C. G. Howes, D. VanInsberghe, H. Yu, D. Bachar, R. Christen, R. Henrik Nilsson, S. J. Hallam, W. W. Mohn, Significant and persistent impact of timber harvesting on soil microbial communities in Northern coniferous forests. *ISME J.* **6**, 2199–2218 (2012).

47. T. Z. DeSantis, P. Hugenholtz, N. Larsen, M. Rojas, E. L. Brodie, K. Keller, T. Huber, D. Dalevi, P. Hu, G. L. Andersen, Greengenes, a chimera-checked 16S rRNA gene database and workbench compatible with ARB. *Appl. Environ. Microbiol.* **72**, 5069–5072 (2006).

48. M. G. Langille, J. Zaneveld, J. G. Caporaso, D. McDonald, D. Knights, J. A. Reyes, J. C. Clemente, D. E. Burkepile, R. L. Vega Thurber, R. Knight, R. G. Beiko, C. Huttenhower, Predictive functional profiling of microbial communities using 16S rRNA marker gene sequences. *Nat. Biotechnol.* **31**, 814–821 (2013).

49. D. H. Parks, G. W. Tyson, P. Hugenholtz, R. G. Beiko, STAMP: Statistical analysis of taxonomic and functional profiles. *Bioinformatics* **30**, 3123–3124 (2014).

50. M. I. Love, W. Huber, S. Anders, Moderated estimation of fold change and dispersion for RNA-seq data with DESeq2. *Genome Biol.* **15**, 550 (2014).

51. Y. Benjamini, Y. Hochberg, Controlling the false discovery rate: A practical and powerful approach to multiple testing. *J. R. Stat. Soc. Ser. B Stat. Methodol.* **57**, 289–300 (1995).

52. J. M. Campbell, G. C. Fahey Jr., B. W. Wolf, Selected indigestible oligosaccharides affect large bowel mass, cecal and fecal short-chain fatty acids, pH and microflora in rats. *J. Nutr.* **127**, 130–136 (1997).

53. A. M. Evans, C. D. DeHaven, T. Barrett, M. Mitchell, E. Milgram, Integrated, nontargeted ultrahigh performance liquid chromatography/electrospray ionization tandem mass spectrometry platform for the identification and relative quantification of the small-molecule complement of biological systems. *Anal. Chem.* **81**, 6656–6667 (2009).

54. C. D. Dehaven, A. M. Evans, H. Dai, K. A. Lawton, Organization of GC/MS and LC/MS metabolomics data into chemical libraries. *J. Cheminform.* **2**, 9 (2010).

55. M. I. Smith, T. Yatsunenko, M. J. Manary, I. Trehan, R. Mkakosya, J. Cheng, A. L. Kau, S. S. Rich, P. Concannon, J. C. Mychaleckyj, J. Liu, E. Houpt, J. V. Li, E. Holmes, J. Nicholson, D. Knights, L. K. Ursell, R. Knight, J. I. Gordon, Gut microbiomes of Malawian twin pairs discordant for kwashiorkor. *Science* **339**, 548–554 (2013).

56. M. R. Blanchet, S. Maltby, D. J. Haddon, H. Merkens, L. Zbytnuik, K. M. McNagny, CD34 facilitates the development of allergic asthma. *Blood* **110**, 2005–2012 (2007).

57. D. Zamar, B. McNeney, J. Graham, elrm: Software implementing exact-like inference for logistic regression models. *J. Stat. Softw.* **21**, 1–18 (2007).

58. M. Plummer, N. Best, K. Cowles, K. Vines, CODA: Convergence diagnosis and output analysis for MCMC. *R News* **6**, 7–11 (2006).

59. R Development Core Team, *R: A Language and Environment for Statistical Computing* (R Foundation for Statistical Computing, Vienna, 2014).

60. P. J. McMurdie, S. Holmes, phyloseq: An R package for reproducible interactive analysis and graphics of microbiome census data. *PLOS One* **8**, e61217 (2013).

61. H. Wickham, *ggplot2: Elegant Graphics for Data Analysis* (Springer-Verlag, New York, 2009).

62. H. Wickham, The split-apply-combine strategy for data analysis. *J. Stat. Softw.* **40**, 1–29 (2011).

63. E. Neuwirth, RColorBrewer: ColorBrewer palettes (2011).

64. J. Oksanen, F. G. Blanchet, R. Kindt, P. Legendre, P. R. Minchin, R. B. O'Hara, G. L. Simpson, P. Solymos, M. Henry, H. Stevens, H. Wagner, vegan: Community ecology package (2013).

65. K. Pollard, H. N. Gilbert, Y. Ge, S. Taylor, S. Dudoit, Multiple testing procedures: R multtest package and applications to genomics, in *Bioinformatics and Computational Biology Solutions Using R and Bioconductor* (Springer, New York, 2005).

66. A. Ploner, Heatplus: Heatmaps with row and/or column covariates and colored clusters (2012).

67. J. Xia, N. Psychogios, N. Young, D. S. Wishart, MetaboAnalyst: A web server for metabolomic data analysis and interpretation. *Nucleic Acids Res.* **37**, W652–W660 (2009).

68. J. Xia, R. Mandal, I. V. Sinelnikov, D. Broadhurst, D. S. Wishart, MetaboAnalyst 2.0—A comprehensive server for metabolomic data analysis. *Nucleic Acids Res.* **40**, W127–W133 (2012).

Science Translational Medicine

Early infancy microbial and metabolic alterations affect risk of childhood asthma

Marie-Claire Arrieta, Leah T. Stiemsma, Pedro A. Dimitriu, Lisa Thorson, Shannon Russell, Sophie Yurist-Doutsch, Boris Kuzeljevic, Matthew J. Gold, Heidi M. Britton, Diana L. Lefebvre, Padmaja Subbarao, Piush Mandhane, Allan Becker, Kelly M. McNagny, Malcolm R. Sears, Tobias Kollmann, the CHILD Study Investigators, William W. Mohn, Stuart E. Turvey and B. Brett Finlay

Window of opportunity for asthma

Changes in the gut microbiota have been implicated in the development of asthma in animal models; however, it has remained unclear whether these findings hold true in humans. Now, Arrieta *et al.* report in a longitudinal human study that infants at risk of asthma have transient gut microbial dysbiosis during the first 100 days of life. They found that certain bacterial genera were decreased in these children. Moreover, adding these bacteria back to germ-free mice decreased airway inflammation, suggesting a potential causative role of the loss of these microbes. They suggest a window where microbe-based diagnostics and therapeutics may be useful to prevent the development of asthma in high-risk individuals.

ARTICLE TOOLS	http://stm.sciencemag.org/content/7/307/307ra152
SUPPLEMENTARY MATERIALS	http://stm.sciencemag.org/content/suppl/2015/09/28/7.307.307ra152.DC1
RELATED CONTENT	http://stm.sciencemag.org/content/scitransmed/7/307/307fs39.full http://stm.sciencemag.org/content/scitransmed/7/301/301ra129.full http://stm.sciencemag.org/content/scitransmed/7/284/284ra60.full http://science.sciencemag.org/content/sci/350/6256/aac5992.full http://stm.sciencemag.org/content/scitransmed/8/321/321ra8.full http://science.sciencemag.org/content/sci/351/6274/672.full http://science.sciencemag.org/content/sci/351/6279/1296.full http://science.sciencemag.org/content/sci/352/6285/530.full http://science.sciencemag.org/content/sci/352/6285/532.full http://science.sciencemag.org/content/sci/352/6285/535.full http://science.sciencemag.org/content/sci/352/6285/539.full http://science.sciencemag.org/content/sci/352/6285/544.full http://science.sciencemag.org/content/sci/352/6285/586.full http://science.sciencemag.org/content/sci/352/6285/560.full http://science.sciencemag.org/content/sci/352/6289/1116.full http://science.sciencemag.org/content/sci/352/6293/1515.full http://science.sciencemag.org/content/sci/352/6293/1581.full http://science.sciencemag.org/content/sci/352/6293/1533.full http://science.sciencemag.org/content/sci/352/6285/565.full
REFERENCES	This article cites 61 articles, 19 of which you can access for free http://stm.sciencemag.org/content/7/307/307ra152#BIBL

Use of this article is subject to the Terms of Service